Supporting Information for "Technical and Economic Irrigation Potentials within land and water boundaries"

Felicitas D. Beier[1,2], Benjamin Leon Bodirsky[1], Jens Heinke[1], Kristine

Karstens[1,2], Jan Philipp Dietrich[1], Christoph Müller[1], Fabian Stenzel[1],

Patrick von Jeetze[1,2], Alexander Popp[1], Hermann Lotze-Campen[1,2]

[1]Potsdam Institute for Climate Impact Research (PIK)

[2]Humboldt-Universität zu Berlin (HU)

Contents of this file

————

Corresponding author: Felicitas D. Beier, Potsdam Institute for Climate Impact Research,

Telegraphenberg A56, 14412 Potsdam, Germany. (beier@pik-potsdam.de)

January 25, 2023, 9:45am

Additional Supporting Information (Files uploaded separately)

1. IrrigationPotentials_global_a.xlsx

2. IrrigationPotentials_global_b.xlsx

3. PIA_bycountry_a.xlsx

4. PIA_bycountry_b.xlsx

5. PIWC_bycountry_a.xlsx

6. PIWC_bycountry_b.xlsx

7. PIWW_bycountry_a.xlsx

8. PIWW_bycountry_b.xlsx

9. Crop_mapping.xlsx

Introduction

This Supporting Information provides additional details to the methods applied in the article.

Additionally, global and country-level results of irrigation potentials (potentially irrigated areas (PIA); potential irrigation water consumption (PIWC); potential irrigation water withdrawals (PIWW)) for 235 countries are provided for two model setups as separate files: (a) under consideration of currently irrigated areas that affect the river flow; (b) not considering currently irrigated areas for irrigation potentials that are purely determined by the economic yield gain ranking.

January 25, 2023, 9:45am

1.   Detailed Methods: LPJmL Model Description

The Lund-Potsdam-Jena managed Land (LPJmL) model is a spatio-temporally explicit process-based model that simulates the growth and geographical distribution of 11 plant functional types (natural vegetation) and 12 crop functional types (field crops) and additionally pasture as well as (woody and herbaceous) bioenergy crops. It accounts for feedbacks between vegetation, the global terrestrial water, carbon, and nitrogen cycles, and energy fluxes and operates at a daily resolution (von Bloh et al., 2018; Schaphoff, von Bloh, et al., 2018; Lutz et al., 2019). The model simulates the terrestrial water balance considering precipitation, snow melt, seepage, interception, plant transpiration and soil evaporation resulting in daily simulations of runoff and discharge and considers its close interactions with plant vegetation in terms of plant growth and productivity that is linked to soil and atmospheric moisture (Schaphoff, Forkel, et al., 2018). It delivers consistent estimates for spatially explicit irrigated and rainfed potential crop yields, plant water uptake and surface runoff that are the basis for our model. Evaporation of irrigation water during the growing season is calculated based on the fraction of irrigation water in soil moisture and canopy interception (Rost et al., 2008). Runoff is the surplus water that cannot be stored in the soil column, after accounting for losses from evapotranspiration.

To determine the structure of the river network in our model, we use the flow direction and stream order of 0.5° grid cells of the global STN-30p drainage network (Vörösmarty et al., 2011); (see also Vörösmarty, Green, Salisbury, and Lammers (2000), Vörösmarty et al. (2011), and Lehner et al. (2011) for a data set description). The drainage network provides for each grid cell the index of the subsequent cell, into which water will be drained,

resulting in a tree-like structure of each river basin, with the estuary as the final cell. It is the same drainage network that is used in the LPJmL simulations used here and is therefore consistent with our hydrological inputs (von Bloh et al., 2018). The underlying land mask used in our study is the 0.5° high-resolution gridded land mask provided by the Climate Research Unit (CRU (Harris et al., 2014, 2020)).

The crop types considered in LPJmL are mapped to the crop types considered in our analysis using the mapping provided in table S1. Since LPJmL considers fewer crops than our analysis, LPJmL's groundnut is also the proxycrop for both oilpalm and cotton; maize is also the proxycrop for fodder (forage) and the 'other' crop category including fruits, vegetables and nuts; temperate roots represent both sugar beet and potatoes.

Irrigated and rainfed crop yields as well as consumptive blue water requirements are provided by LPJmL5 with unlimited nitrogen supply (von Bloh et al., 2018). As opposed to previous LPJmL versions (Sitch et al., 2003; Bondeau et al., 2007; Schaphoff, von Bloh, et al., 2018; Schaphoff, Forkel, et al., 2018), LPJmL5 includes an implementation of the global terrestrial nitrogen cycle and consistently accounts for water, grassland and crop management. Since the LPJmL4 and LPJmL5 model version have diverged during the Nitrogen cycle implementation phase, certain natural vegetation dynamics (Forkel et al., 2014) have not yet been included in the newest LPJmL5 version (von Bloh et al., 2018). For this reason, natural vegetation inputs, such as lake evaporation, runoff and monthly discharge are provided by its predecessor LPJmL4 (Schaphoff, von Bloh, et al., 2018; Schaphoff, Forkel, et al., 2018).

2. Detailed Methods: Yield Gain Potential

LPJmL models crop growth under rainfed and irrigated conditions for different growing periods based on crop calendars developed within phase 3 of the Global Gridded Crop Model Intercomparison Project (Jägermeyr et al., 2021). It therefore considers shifts in the growing period through irrigation. The difference of irrigated and rainfed crop yields as estimated by LPJmL provides the yield gain through irrigation in tons of dry matter.

To account for country-specific management effects on yields (e.g. fertilizer and pesticide use; different crop varieties; mechanization; cropping intensity representing multiple cropping or fallow land), LPJmL potential yields are calibrated to meet country-level production as reported by FAO (FAO, 2021) using the same multiplicative factor for both rainfed and irrigated yields. A potential multiple cropping effect is therefore applied to both irrigated and rainfed yields and cannot capture the effect that irrigation may lead to an additional cropping season and increase yields by one or two additional harvests per year.

Figure S1a shows the average rainfed yield of the chosen crop mix in 2010 in USD per hectare. Figure S1b shows the potential yield gain through irrigation in USD per hectare for the chosen crop mix in 2010. It represents the areas that would achieve yield gains through irrigation considering irrigated and rainfed potential yields valued at global FAO average prices (in USD per tDM). We use country-level annual producer prices as provided by FAOSTAT (FAO, 2021), map the FAO production items to the crop types used in our study (see table Crop_mapping.xlsx), and calculate global average prices using production quantity as aggregation and averaging weight to ensure international comparability.

January 25, 2023, 9:45am

The average rainfed yield on currently irrigated areas is 1946 USD ha^{-1}. On the same areas, an average irrigated yield of 3091 USD ha^{-1} is achieved.

The average yield gain on currently irrigated areas is 1056 USD ha^{-1}. Taking only those areas into account where sufficient local water resources are available, the yield gain on currently irrigated areas is 867 USD ha^{-1}. On all of current cropland (rainfed and irrigated), the average yield gain is 596 USD ha^{-1} and 446 USD ha^{-1} where sufficient local water resources are available. On total potential cropland, the average yield gain is 840 USD ha^{-1} and 357 USD ha^{-1} where sufficient local water resources are available.

As sensitivity check for the obtained yield gains, we tested two alternative price scenarios against the chosen global average commodity prices: country-specific crop commodity prices and a hypothetical single global commodity price of 571 USD ha^{-1} (average yield gain). The spatial patterns of yield gains are largely identical to the pattern shown in figure S1. The Spearman's rank correlation rho between the grid cell specific yield gains in the global average commodity price valuation compared to the grid cell specific yield gain with country-specific commodity prices is 0.9892 (see figure S2b). The Sperman's rank correlation rho between the global average commodity price valued yield gain and the yield gain at an hypothetical global single commodity price of 571 USD ha^{-1} for all crops is still 0.9831. This shows that the spatial patterns of the yield gain (and therefore also spatial patterns of irrigation potentials) are for the most part driven by differences in the crop yield gain through irrigation in tons dry matter, not the price scenario. The price valuation is, however, necessary to determine where irrigation is beneficial under different thresholds. The potentially irrigated area that falls into each threshold category in the different scenarios is shown in figure S2.

3.   Detailed Methods: Irrigation Costs

Given the lack of spatially explicit irrigation cost data and uncertainty with respect to exchange rates, interest rates and regional differences, we choose a medium threshold of $300\,\text{USD}\,\text{ha}^{-1}$ representing the lower end of infrastructure investment costs of new constructions; and a high threshold of $600\,\text{USD}\,\text{ha}^{-1}$. They are meant to represent a plausible range based on the average annuities of irrigation cost data found in the literature.

The IWMI research report by Inocencio, Institute, and (Program) (2007) reports average unit cost of irrigation projects for a sample of 50 developing countries. They find average unit costs for new construction of $8213\,\text{USD}\,\text{ha}^{-1}$ across all regions. At a $4\,\%$ interest rate, this corresponds to an annuity of $316\,\text{USD}\,\text{ha}^{-1}$ and at an interest rate of $8\,\%$ to $608\,\text{USD}\,\text{ha}^{-1}$.

In addition to infrastructure investment costs, there are Operation and Management (O&M) costs involved in irrigation (D'Odorico et al., 2020; You et al., 2011). The assumed fixed infrastructure investment costs and O&M costs in You et al. (2011) result in annuities between 44-$370\,\text{USD}\,\text{ha}^{-1}$ for small-scale projects, and 222-$592\,\text{USD}\,\text{ha}^{-1}$ for large-scale projects. These numbers are obtained by calculating the annuity of the fixed investment costs using an interest rate of $8\,\%$ and adding annual O&M costs, both of which are estimated from literature values in You et al. (2011).

4.   Detailed Methods: Currently Irrigated Area and Irrigation Water Use

To derive the grid cell area (in Mha) that was irrigated in the year 2010, we use the irrigated area share provided by the Land-Use Harmonization 2 (LUH2) data set presented in Hurtt et al. (2020) (Hurtt et al., 2019, 2020). LUH2 is based on the HYDE 3.2 data set (Klein Goldewijk et al., 2017) that estimates historically irrigated areas based on Siebert

et al. (2015), Portmann, Siebert, and Döll (2010) and FAOSTAT data (FAO, 2021). The LUH2 cropland map is subdivided into only five crop functional types (C3 annuals; C4 annuals; C3 perennials; C4 perennials; C3 nitrogen fixers). These five functional types are further disaggregated into 17 crop groups using relative shares of area harvested on country level from FAOSTAT. The mapping of FAOSTAT production items and LUH2 crop classes to our crop categories is provided in the Crop_mapping.xlsx table.

LUH2 further contains flooded area shares and in our crop categories only rice is flooded. We therefore determine the distribution of physical rice areas by assigning the country's rice production first to flooded areas provided at cellular level by LUH2. Upland (aerobic) rice is accounted by distributing country-level FAO rice areas beyond country-aggregated LUH2 flooded area (i.e. where FAO reports higher country-level rice areas than there are LUH2 flooded areas in the respective country) equally across the remaining country's cropland area of C3 annual crops.

Given the area irrigated and the crop pattern in 2010 derived from LUH2 and FAO-STAT, the volume of current cellular irrigation water use ($U_{c,w}$) is calculated by

$$U_{c,w} = \sum_k V_{c,k,w} \cdot A_{c,k} \tag{1}$$

$V_{c,k,w}$ refer to the crop water requirements per crop type (k) and grid cell (c) for the two water use types (w = consumption and withdrawal), $A_{c,k}$ is the irrigated area per grid cell and crop. Grid cell specific crop water requirements further depend on the irrigation system in use. We use country-level irrigation system shares provided by Jägermeyr et al. (2015) and assign grid cell specific irrigation system shares using the cellular crop mix assumed throughout the study and crop-specific irrigation system suitability provided by

Jägermeyr et al. (2015). For the crop categories 'Fruits, Vegetables, Nuts', 'Oilpalm', 'Tropical roots (incl. cassava)', 'Potato' and 'Cotton', we assumed that all irrigation systems are suitable.

5. Detailed Methods: Environmental Flow Requirements and Accessibility Restrictions

The share of yearly discharge to be reserved for EFR per grid cell is calculated over a long-term reference period (1985-2015) based on monthly discharge provided by LPJmL4 (Schaphoff, von Bloh, et al., 2018). For a functioning freshwater ecosystem, a certain base flow (low flow requirements, LFR) is necessary to avoid aquatic species loss. Additionally, flooding plays an important role for riverine vegetation and wetlands. It can be accounted for by high flow requirements (HFR) (Smakhtin et al., 2004). We follow the Variable Monthly Flow (VMF) method introduced by Pastor, Ludwig, Biemans, Hoff, and Kabat (2014). It determines EFR using the flow variation throughout a year with different requirements for low-, intermediate- and high-flow months parametrized to a 'fair' ecosystem preservation status. In low-flow months (i.e. months in which mean monthly flow is smaller or equal to 40 % of the mean annual flow), 60 % of mean monthly flows are reserved for the environment; in intermediate-flow months (i.e. months in which mean monthly flow is greater than 40 %, but smaller than 80 % of the mean annual flow) 45 %; and in high-flow months (i.e. months in which mean monthly flow is greater than 80 % of the mean annual flow) 30 % of mean monthly flows is reserved (Pastor et al., 2014). We adopted this method by splitting EFR into LFR and HFR-equivalents. Discharge reserved in low-flow months is attributed to LFR, discharge reserved in high-flow months is attributed to HFR, and half of intermediate-flow requirements are attributed to LFRs and

the other half to HFRs to appropriately consider the interaction of EFR and inaccessible discharge.

Not all water on Earth can easily be brought into productive usage (Postel et al., 1996; de Fraiture et al., 2001). Especially highly variable flows are difficult to access for humans and could only be used for irrigation with appropriate storage infrastructure (reservoirs), which are costly to install. To account for such inaccessible (or hardly accessible) discharge, we use the coefficient of variation (CV) of monthly discharge as described in the main text.

With the monthly discharge time series provided by LPJmL4, the CV $\left(\frac{\sigma_c}{\mu_c}\right)$ ranges between 0 and 19.11 resulting in a functional form as displayed in figure S3b. The bulk of the data lies between 0 and 3.61 with the 25th percentile at 1.08 and the 75th percentile at 2.09 (see figure S3a).

We assume that seasonally highly variable flows are difficult to access by humans, but may serve an ecosystem function similar to HFRs. The baseflow or LFR, on the other hand, cannot be served by such variable flows and must be left untouched by human intervention when the environmental flow protection is considered. For this reason, we split discharge reserved for EFR into HFRs and LFRs. When discharge is constrained based on the accessibility constraint, HFRs count towards the inaccessible discharge, while LFRs are excluded from human access in addition to inaccessible discharge.

6. Scenario Details: Natural Land Protection

Figure S4 shows areas of ecological importance following the Half-Earth protection approach based on the data provided by Kok et al. (2020). It puts at least 50 % of the land surface of each 'ecoregion', as described in Dinerstein et al. (2019), under protection.

This includes currently protected areas based on the World Database of Protected Areas (WDPA), biodiversity hotspots (Mittermeier et al., 2005) and intact forest landscapes (Potapov et al., 2017).

7.   Extended Discussion: The Assumption of Full Irrigation

The irrigation water requirements provided by LPJmL represent 'full irrigation water requirements', i.e. the water required by a crop so that no water limitation occurs. In reality, in areas where water supply is limited and the marginal cost for water is high, deficit irrigation is applied (Geerts & Raes, 2009). A comprehensive coverage of deficit irrigation would require establishing a marginal yield-water response curve showing the relationship between water requirements and yields for each crop in each cell. Such water production functions are non-linear and differ by crop- and genotype, phenological stage and location (climate, soil) (Geerts & Raes, 2009). Furthermore, the 'optimum' deficit water use level differs depending on whether water or land is the limiting factor and are subject to uncertainties (weather, soil conditions, pests and diseases, use of chemicals and fertilizer) (English, 1990). While the opportunity cost of an additional drop of water may be the most important decision criterion where water availability is limited and the water saved by deficit irrigation in one location would enable the irrigation of additional land (English, 1990), this additional land would also have to be connected to irrigation infrastructure (e.g., canals) and equipped with irrigation equipment (e.g., pumps and irrigation system equipment), which involves additional costs. High water costs would incentivize deficit irrigation, while high fixed costs for conveyance canals and sprinklers incentivize full irrigation. A comprehensive assessment of deficit irrigation would therefore also require spatially explicit information on the relative difference between variable water

costs and fixed investment costs. All of these aspects differ depending on the spatial location and cannot be captured appropriately in a global-scale model. Moreover, a hierarchical ranking in water allocation between cells would not be possible anymore. All cells would need to adjust their degree of deficit irrigation simultaneously. Therefore, the water allocation could not be derived iteratively, but only simultaneously for all cells.

References

Bondeau, A., Smith, P. C., Zaehle, S., Schaphoff, S., Lucht, W., Cramer, W., ... Smith, B. (2007, March). Modelling the role of agriculture for the 20th century global terrestrial carbon balance. *Global Change Biology*, *13*(3), 679–706. Retrieved 2020-10-04, from `http://doi.wiley.com/10.1111/j.1365-2486.2006.01305.x` doi: 10.1111/j.1365-2486.2006.01305.x

de Fraiture, C., Molden, D., Amarasinghe, U., & Makin, I. (2001, January). PODIUM: Projecting water supply and demand for food production in 2025. *Physics and Chemistry of the Earth, Part B: Hydrology, Oceans and Atmosphere*, *26*(11-12), 869–876. Retrieved 2021-01-07, from `https://linkinghub.elsevier.com/retrieve/pii/S1464190901000995` doi: 10.1016/S1464-1909(01)00099-5

Dinerstein, E., Vynne, C., Sala, E., Joshi, A. R., Fernando, S., Lovejoy, T. E., ... Wikramanayake, E. (2019, April). A Global Deal For Nature: Guiding principles, milestones, and targets. *Science Advances*, *5*(4), eaaw2869. Retrieved 2021-12-10, from `https://www.science.org/doi/10.1126/sciadv.aaw2869` doi: 10.1126/sciadv.aaw2869

D'Odorico, P., Chiarelli, D. D., Rosa, L., Bini, A., Zilberman, D., & Rulli, M. C. (2020, September). The global value of water in agriculture. *PNAS*, *117*(36), 21985–21993.

English, M. (1990, May). Deficit Irrigation. I: Analytical Framework. *Journal of Irrigation and Drainage Engineering*, *116*(3), 399–412. Retrieved 2022-06-13, from `https://ascelibrary.org/doi/10.1061/%28ASCE%290733-9437%281990%29116%3A3%28399%29` doi: 10.1061/(ASCE)0733-9437(1990)116:3(399)

FAO. (2021). *FAOSTAT Data* [Bulk Download]. Retrieved 2021-05-21, from `http://`

www.fao.org/faostat/en/

Forkel, M., Carvalhais, N., Schaphoff, S., v. Bloh, W., Migliavacca, M., Thurner, M.,
    & Thonicke, K. (2014, December). Identifying environmental controls on vegeta-
    tion greenness phenology through model–data integration. *Biogeosciences*, *11*(23),
    7025–7050. Retrieved 2021-09-27, from `https://bg.copernicus.org/articles/`
    `11/7025/2014/` doi: 10.5194/bg-11-7025-2014

Geerts, S., & Raes, D. (2009, September). Deficit irrigation as an on-farm strategy
    to maximize crop water productivity in dry areas. *Agricultural Water Management*,
    96(9), 1275–1284. Retrieved 2022-06-19, from `https://linkinghub.elsevier.com/`
    `retrieve/pii/S0378377409001243` doi: 10.1016/j.agwat.2009.04.009

Harris, I., Jones, P., Osborn, T., & Lister, D. (2014, March). Updated high-resolution
    grids of monthly climatic observations - the CRU TS3.10 Dataset: UPDATED HIGH-
    RESOLUTION GRIDS OF MONTHLY CLIMATIC OBSERVATIONS. *Interna-
    tional Journal of Climatology*, *34*(3), 623–642. Retrieved 2021-12-21, from `https://`
    `onlinelibrary.wiley.com/doi/10.1002/joc.3711` doi: 10.1002/joc.3711

Harris, I., Osborn, T. J., Jones, P., & Lister, D. (2020, December). Version 4 of the
    CRU TS monthly high-resolution gridded multivariate climate dataset. *Scientific
    Data*, *7*(1), 109. Retrieved 2021-12-21, from `http://www.nature.com/articles/`
    `s41597-020-0453-3` doi: 10.1038/s41597-020-0453-3

Hurtt, G. C., Chini, L., Sahajpal, R., Frolking, S., Bodirsky, B. L., Calvin, K., . . .
    Zhang, X. (2019). Harmonization of Global Land Use Change and Management for
    the Period 850-2015. *Earth System Grid Federation*. doi: https://doi.org/10.22033/
    ESGF/input4MIPs.10454

Hurtt, G. C., Chini, L., Sahajpal, R., Frolking, S., Bodirsky, B. L., Calvin, K., ... Zhang, X. (2020, November). Harmonization of global land use change and management for the period 850–2100 (LUH2) for CMIP6. *Geoscientific Model Development*, *13*(11), 5425–5464. Retrieved 2021-09-24, from `https://gmd.copernicus.org/articles/13/5425/2020/` doi: 10.5194/gmd-13-5425-2020

Inocencio, A. B., Institute, I. W. M., & (Program), F. H. (Eds.). (2007). *Costs and performance of irrigation projects: a comparison of Sub-Saharan Africa and other developing regions* (No. 109). Colombo: International Water Management Institute.

Jägermeyr, J., Gerten, D., Heinke, J., Schaphoff, S., Kummu, M., & Lucht, W. (2015, July). Water savings potentials of irrigation systems: global simulation of processes and linkages. *Hydrology and Earth System Sciences*, *19*(7), 3073–3091. Retrieved 2018-10-04, from `https://www.hydrol-earth-syst-sci.net/19/3073/2015/` doi: 10.5194/hess-19-3073-2015

Jägermeyr, J., Müller, C., Minoli, S., Ray, D., & Siebert, S. (2021). *GGCMI Phase 3 crop calendar.* https://doi.org/10.5281/zenodo.5062513. Retrieved from `https://doi.org/10.5281/zenodo.5062513`

Klein Goldewijk, K., Beusen, A., Doelman, J., & Stehfest, E. (2017, December). Anthropogenic land use estimates for the Holocene – HYDE 3.2. *Earth System Science Data*, *9*(2), 927–953. Retrieved 2021-09-24, from `https://essd.copernicus.org/articles/9/927/2017/` doi: 10.5194/essd-9-927-2017

Kok, M. T., Meijer, J. R., van Zeist, W.-J., Hilbers, J. P., Immovilli, M., Janse, J. H., ... Alkemade, R. (2020, August). *Assessing ambitious nature conservation strategies within a 2 degree warmer and food-secure world* (preprint). Ecology. Retrieved 2021-

11-30, from `http://biorxiv.org/lookup/doi/10.1101/2020.08.04.236489` doi: 10.1101/2020.08.04.236489

Lehner, B., Liermann, C. R., Revenga, C., Vörösmarty, C., Fekete, B., Crouzet, P., . . . Wisser, D. (2011, November). High-resolution mapping of the world's reservoirs and dams for sustainable river-flow management. *Frontiers in Ecology and the Environment*, *9*(9), 494–502. Retrieved 2021-06-22, from `https://onlinelibrary.wiley.com/doi/abs/10.1890/100125` doi: 10.1890/100125

Lutz, F., Herzfeld, T., Heinke, J., Rolinski, S., Schaphoff, S., von Bloh, W., . . . Müller, C. (2019, June). Simulating the effect of tillage practices with the global ecosystem model LPJmL (version 5.0-tillage). *Geoscientific Model Development*, *12*(6), 2419–2440. Retrieved 2021-11-12, from `https://gmd.copernicus.org/articles/12/2419/2019/` doi: 10.5194/gmd-12-2419-2019

Mittermeier, R. A., Robles Gil, P., Michael, H., Pilgrim, J., Brooks, T., Goettsch Mittermeier, C., . . . da Fonseca, G. A. B. (2005). *Hotspots Revisited: Earth's Biologically Richest and Most Endangered Terrestrial Ecoregions* (2nd ed., Vol. 12). Conservation International.

Pastor, A. V., Ludwig, F., Biemans, H., Hoff, H., & Kabat, P. (2014, December). Accounting for environmental flow requirements in global water assessments. *Hydrology and Earth System Sciences*, *18*(12), 5041–5059. Retrieved 2020-12-15, from `https://hess.copernicus.org/articles/18/5041/2014/` doi: 10.5194/hess-18-5041-2014

Portmann, F. T., Siebert, S., & Döll, P. (2010, March). MIRCA2000-Global monthly irrigated and rainfed crop areas around the year 2000: A new high-resolution data set for agricultural and hydrological modeling: MONTHLY IRRIGATED AND

RAINFED CROP AREAS. *Global Biogeochemical Cycles*, *24*(1), n/a–n/a. Retrieved 2021-09-25, from `http://doi.wiley.com/10.1029/2008GB003435` doi: 10.1029/2008GB003435

Postel, S. L., Daily, G. C., & Ehrlich, P. R. (1996, February). Human Appropriation of Renewable Fresh Water. *Science*, *271*(5250), 785–788. Retrieved 2021-12-23, from `https://www.science.org/doi/10.1126/science.271.5250.785` doi: 10.1126/science.271.5250.785

Potapov, P., Hansen, M. C., Laestadius, L., Turubanova, S., Yaroshenko, A., Thies, C., ... Esipova, E. (2017, January). The last frontiers of wilderness: Tracking loss of intact forest landscapes from 2000 to 2013. *Science Advances*, *3*(1), e1600821. Retrieved 2021-12-19, from `https://www.science.org/doi/10.1126/sciadv.1600821` doi: 10.1126/sciadv.1600821

Rost, S., Gerten, D., Bondeau, A., Lucht, W., Rohwer, J., & Schaphoff, S. (2008, September). Agricultural green and blue water consumption and its influence on the global water system: GLOBAL WATER USE IN AGRICULTURE. *Water Resources Research*, *44*(9). Retrieved 2021-04-19, from `http://doi.wiley.com/10.1029/2007WR006331` doi: 10.1029/2007WR006331

Schaphoff, S., Forkel, M., Müller, C., Knauer, J., von Bloh, W., Gerten, D., ... Waha, K. (2018, April). LPJmL4 – a dynamic global vegetation model with managed land – Part 2: Model evaluation. *Geoscientific Model Development*, *11*(4), 1377–1403. Retrieved 2021-09-03, from `https://gmd.copernicus.org/articles/11/1377/2018/` doi: 10.5194/gmd-11-1377-2018

Schaphoff, S., von Bloh, W., Rammig, A., Thonicke, K., Biemans, H., Forkel, M., ...

Waha, K. (2018, April). LPJmL4 – a dynamic global vegetation model with managed land – Part 1: Model description. *Geoscientific Model Development*, *11*(4), 1343–1375. Retrieved 2021-09-03, from `https://gmd.copernicus.org/articles/11/1343/2018/` doi: 10.5194/gmd-11-1343-2018

Siebert, S., Kummu, M., Porkka, M., Döll, P., Ramankutty, N., & Scanlon, B. (2015). *Historical Irrigation Dataset (HID)*. MyGeoHUB. Retrieved 2021-09-25, from `https://mygeohub.org/publications/8/2` (Type: dataset) doi: 10.13019/M20599

Sitch, S., Smith, B., Prentice, I. C., Arneth, A., Bondeau, A., Cramer, W., . . . Venevsky, S. (2003, February). Evaluation of ecosystem dynamics, plant geography and terrestrial carbon cycling in the LPJ dynamic global vegetation model: LPJ DYNAMIC GLOBAL VEGETATION MODEL. *Global Change Biology*, *9*(2), 161–185. Retrieved 2021-09-27, from `http://doi.wiley.com/10.1046/j.1365-2486.2003.00569.x` doi: 10.1046/j.1365-2486.2003.00569.x

Smakhtin, V., Revenga, C., & Döll, P. (2004, September). A Pilot Global Assessment of Environmental Water Requirements and Scarcity. *Water International*, *29*(3), 307–317. Retrieved 2020-12-15, from `http://www.tandfonline.com/doi/abs/10.1080/02508060408691785` doi: 10.1080/02508060408691785

von Bloh, W., Schaphoff, S., Müller, C., Rolinski, S., Waha, K., & Zaehle, S. (2018). Implementing the nitrogen cycle into the dynamic global vegetation, hydrology, and crop growth model LPJmL (version 5.0). *Geoscientific Model Development*, *11*(7), 2789–2812. Retrieved 2021-11-10, from `https://gmd.copernicus.org/articles/11/2789/2018/` doi: 10.5194/gmd-11-2789-2018

Vörösmarty, C. J., Fekete, B. M., Hall, F. G., Collatz, G. J., Meeson, B. W., Los, S. O., . . . Landis, D. R. (2011). *ISLSCP II River Routing Data (STN-30p).* ORNL DAAC. Retrieved from `https://doi.org/10.3334/ORNLDAAC/1005`

Vörösmarty, C. J., Green, P., Salisbury, J., & Lammers, R. B. (2000, July). Global Water Resources: Vulnerability from Climate Change and Population Growth. *Science*, *289*(5477), 284–288. Retrieved 2018-06-04, from `http://www.sciencemag.org/cgi/doi/10.1126/science.289.5477.284` doi: 10.1126/science.289.5477.284

You, L., Ringler, C., Nelson, G. C., Wood-Sichra, U., Robertson, R. D., Wood, S., . . . Sun, Y. (2011). What is the irrigation potential for Africa? A combined biophysical and socioeconomic approach. *Food Policy*, *36*(2011), 770–782.

Crop types considered in LPJmL	Crop types considered in this study
Temperate cereals	Temperate cereals
Tropical cereals	Tropical cereals
Maize	Maize; Others (fruits, vegetable, nuts); Forage
Rice	Rice
Oil crops (soybean)	Soybean
Oil crops (rapeseed)	Other oil crops (including rapeseed)
Oil crops (groundnut)	Groundnuts; Oilpalms; Cotton
Oil crops (sunflower)	Sunflower
Pulses	Pulses
Temperate roots	Potatoes; Sugar beet
Tropical roots	Tropical roots (including cassava)
Sugar cane	Sugar cane

Table S1.   Mapping of LPJmL crop types to crop types considered in our analysis.

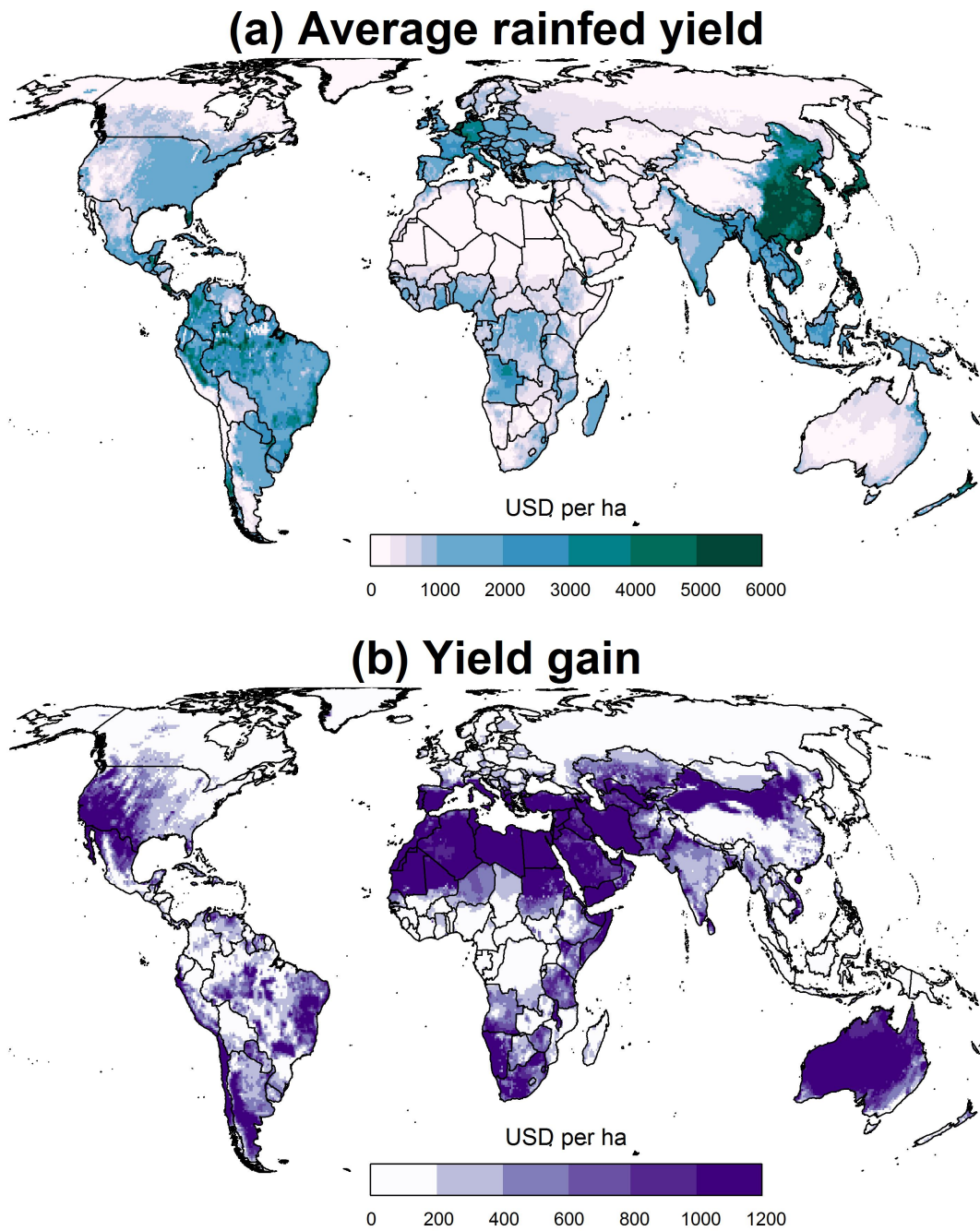## (a) Average rainfed yield

(b) Yield gain

Figure S1. (a) Average rainfed yield on potential cropland (2010) and (b) Potential yield gain through irrigation (2010) in USD ha^{-1}.
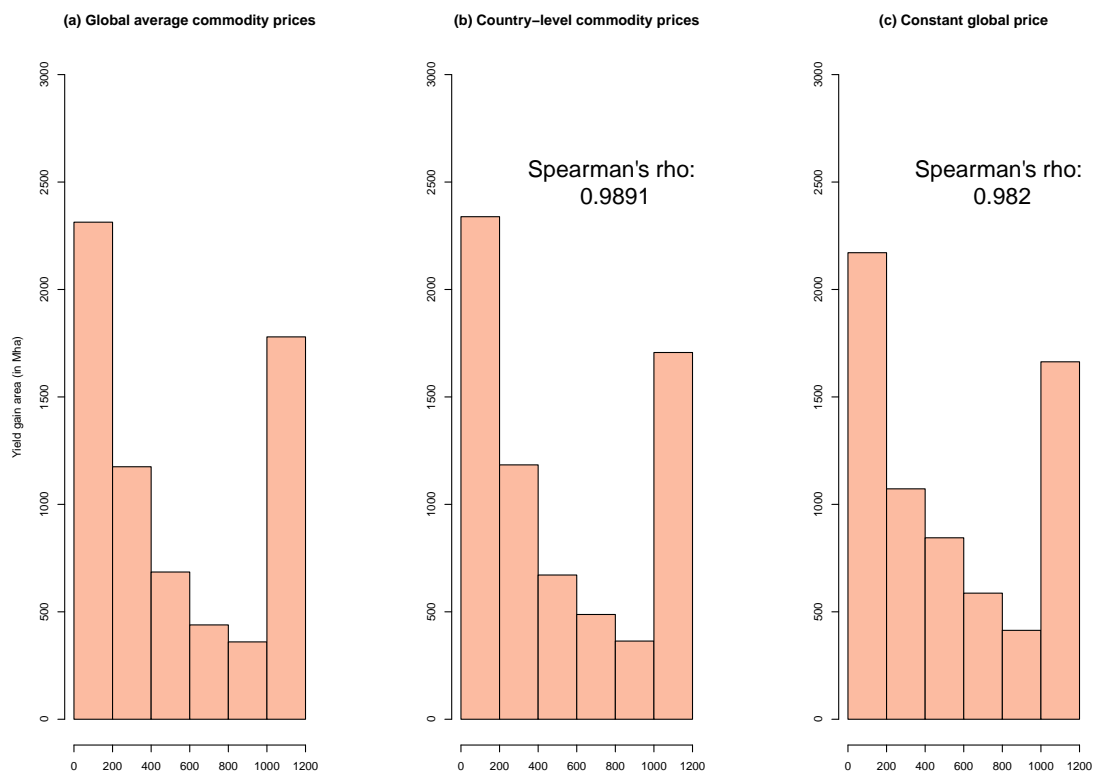
Figure S2. Area-weighted histogram of yield gains (in 2010) at different price scenarios: (a) global average crop commodity prices; (b) country-specific crop commodity prices; (c) global single commodity price.
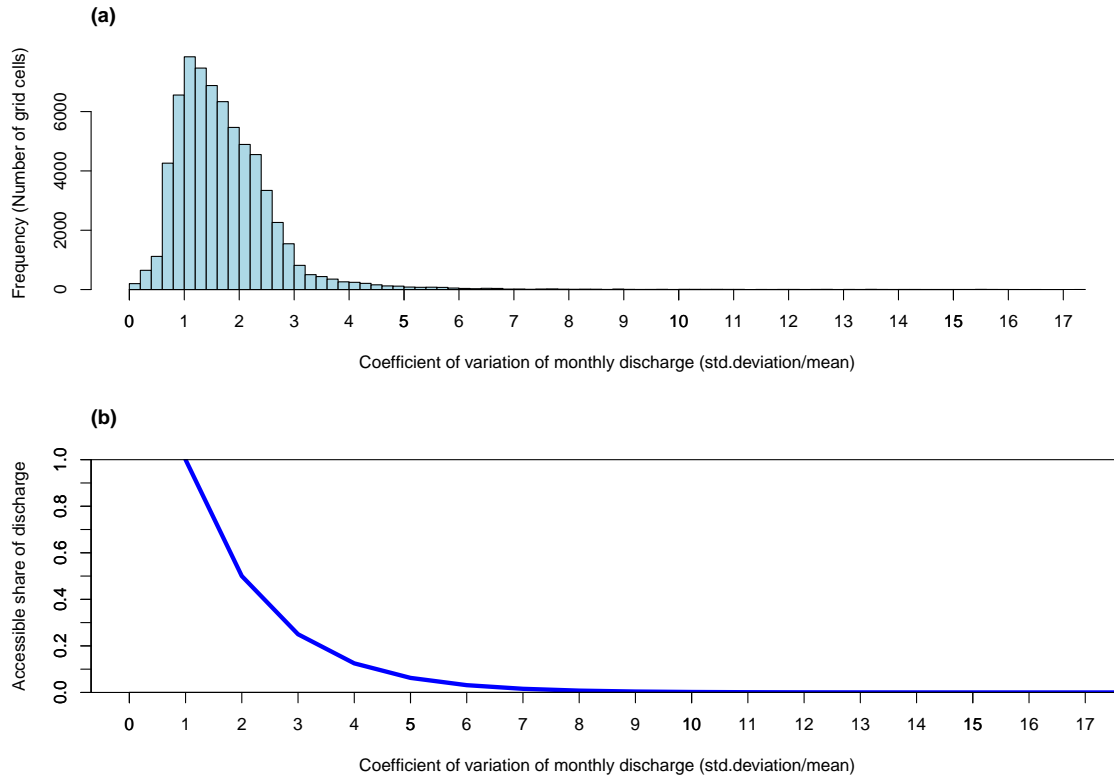
(a)

(b)

Figure S3. Frequency of Coefficient of Variation (CV) of monthly discharge (a) and functional relationship between discharge accessibility share and CV of monthly discharge (b) for time series of monthly discharge over the period from 1980 to 2010.
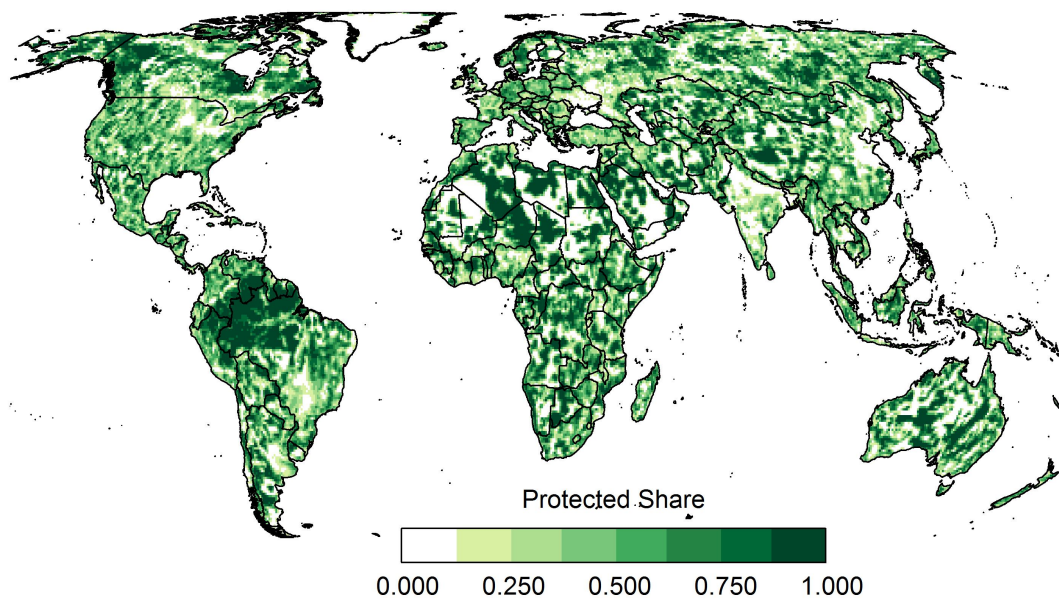
January 25, 2023, 9:45am

Figure S4.   Share of grid cell that would be protected according to the Half-Earth

protection approach.